CONTROLLED GROWTH OF HYDROXYAPATITE IN THE PRESENCE OF SPECIFIC BINDING PEPTIDES

TREBALL DE FI DE GRAU

Marta Mercè Minguet

Dirigit per la Prof. Carole Perry

UNIVERSITAT ROVIRA I VIRGILI

Nottingham, Maig 2016

ACKNOWLEDGEMENTS

I would like to express my gratitude to all people who helped me during this project. First of all, to Carole Perry who gave me this opportunity to improve my scientific knowledge in the United Kingdom. And especially to Robyn and David who were always available to give me advice and assist.

I would also like to thank my friends in Nottingham who cheered me up when I did not obtain the results that I expected.

Finally, I would like to appreciate all the support received from my family and my friends from Catalonia.

INDEX

ABSTRACT

Hydroxyapatite (HAp) materials have been an important area of development in the last decades due to their biomedical application as it is the main inorganic compound of bone. This current study tries to investigate the different effects of peptides binding to HAp.

Four peptides known to promote HAp formation (CaP(V)-VTKHLNQISQSY, CaP(A)-APWHLSSQYSRT, CaP(S)-STLPIPHEFSRE, CaP(H)-SVSVGMKPSPRP) were successfully synthesised. Two wet chemical methods were explored for HAp growth. In *method 1*, calcium phosphate with the target phase (HAp) was obtained. However, in *method 2*, HAp was not obtained, instead the Brushite phase formed.

CaP(V), CaP(A) and CaP(S), are the peptides that favoured the formation of HAp without the presence of other phases. CaP(H) results were not reproducible.

Due to there being no significant differences in X-Ray Diffraction data, no conclusions were reached about the effects of each peptide.

1. INTRODUCTION

1.1. Area of development

This work has taken place in the Biomolecular Materials Interface Research Group at Nottingham Trent University (NTU). The group is working on different projects, all of them to understand what happens at the interface between biomolecules and materials with the aim of producing a set of rules that can be used predictively with other materials systems.[1] The group is headed by Pr. Carole Perry and throughout this project I had two supervisors: Robyn Plowright who is doing her PhD and David Belton who is a research fellow in the group.

1.2. Introduction

During the past decades, there have been major advances in the development of biomedical materials including various ceramic materials for skeletal repair and reconstruction. This is an important aspect considering the resulting increase in life expectancy and quality of life.[2] The aim of bone tissue engineering is the development of a construct which is implanted in the body and performs the function of bones, both on the cellular and structural levels without causing immune reactions and allowing adequate natural tissue ingrowth. The ideal treatment would be one that improves and imitates the body's natural response facing the injury in the bone, using biomolecules or growth factors and cells, resulting in natural bone growth at the site of damage.

Bone is a living tissue composed of minerals, protein, water, cells and other macromolecules. Bone minerals constitute 2/3 part of the total volume of bone and is essentially composed of Hydroxyapatite (HAp)[3], the principal inorganic constituent and the aim of this project.

The responsible cells for the formation of bone matrix are the osteoblasts, these cells are recruited and head towards the place of bone formation, where they are responsible for synthesizing, segregating, organization and mineralization of the bone matrix.[4] This formation is possible due to the interaction of proteins during calcium phosphate crystallisation in HAp. An important factor for controlling nucleation is the interaction of proteins, it is demonstrated that peptides influence the rate, morphology, and polymorph development during crystallization.[5,6,7]

To identify peptide sequences that preferentially bind to apatite-based substrates techniques such as phage display, enzyme-linked immunosorbant assay (ELISA) and computational molecular modelling can be used. Phage display (Ph.D.)is a laboratory technique for identifying peptide sequences that bind to proteins, DNA, cells,

polymers, and even inorganic materials such as silver and titanium.[8] Ph.D. works by using a library of peptide or protein variants expressed on the outside of a phage virion, while the genetic material encoding each variant resides on the inside. This creates a physical linkage between each variant protein sequence and the DNA encoding it, which allows rapid partitioning based on binding affinity to a given target molecule (*figure 1*).[9]

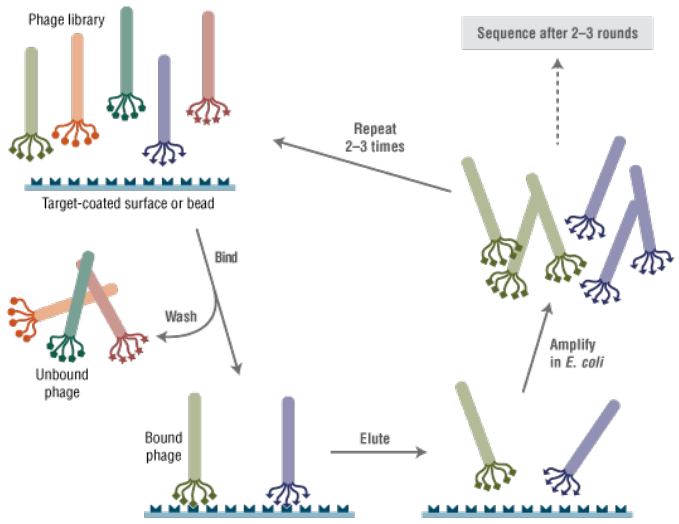

Figure 1.Phage display selection scheme for the identification of the peptides with high affinity.[9]

The four peptides studied are shown in the following table (*table 1*):

Table 1. Propound peptides for the work

Name	Sequence	Reference
CaP(V)	VTKHLNQISQSY	10,11
CaP(A)	APWHLSSQYSRT	10,11
CaP(S)	STLPIPHEFSRE	10,11
CaP(H)	SVSVGMKPSPRP	5,6

1.3. Hydroxyapatite

HAp, is a bioactive ceramic that has been highly favoured in surgical reconstruction of bones owing to it is osteoconductivity, biocompatibility and biodegradability.[12] For this reason, it has widely been investigated.

- Osteoconductivity: the ability of the bone to grow on the contact surface.
- Biocompatibility: the capability of coexistence with living tissues or organisms without causing harm.
- Biodegradability: the capability of decaying through the action of living organisms. A biodegradable material is nontoxic and it dissolves when placed in biological environment.

HAp is one of many calcium phosphate crystalline structures (*table 2*), the formula of this mineral is, $Ca_{10}(PO_4)_6OH_2$.[2]

Table 2. Summary of crystalline calcium phosphate phases.[13]

Abbreviation	Formula	Name (mineral)
HAp	$Ca_{10}(PO_4)_6(OH)_2$	Hydroxyapatite
OCP	$Ca_8H_2(PO_4)_6{\cdot}5H_2O$	Octacalcium phosphate
β-TCP	$Ca_3(PO_4)_2$	β-Tricalcium phosphate (whitlockite)
α-TCP	$Ca_3(PO_4)_2$	α-Tricalcium phosphate
ACP	$Ca_x(PO_4)_y{\cdot}nH_2O$	Amorphous calcium phosphate
MCPM	$Ca(H_2PO_4)_2{\cdot}H_2O$	Monocalcium phosphate monohydrate
MCPA	$Ca(H_2PO_4)_2$	Anhydrous monocalcium phosphate
DCPD	$CaHPO_4{\cdot}2H_2O$	Dicalcium phosphate dehydrates (brushite)
DCPA	$CaHPO_4$	Anhydrous dicalcium phosphate (monetite)
TTCP	$Ca_4(PO_4)_2$	Tetracalcium phosphate
CDHA	$Ca_{10-x}(HPO_4)_x(PO4)_{6-x}(OH)_{2-x}$	Calcium-deficient hydroxyapatite

HAp has a hexagonal structure with $P6_3/m$ space group and cell dimension a=b=9,42Å and c=6,88Å. It has a stoichiometric Ca/P ratio of 1,67. It contains two different cations sites: Ca(I) and Ca(II), among 10 cations, the 4 Ca(I) are tightly bonded to 6 oxygens and less strongly to the other 3 oxygens, whereas the 6 Ca(II) atoms are surrounded by 7 oxygens.[12,13]

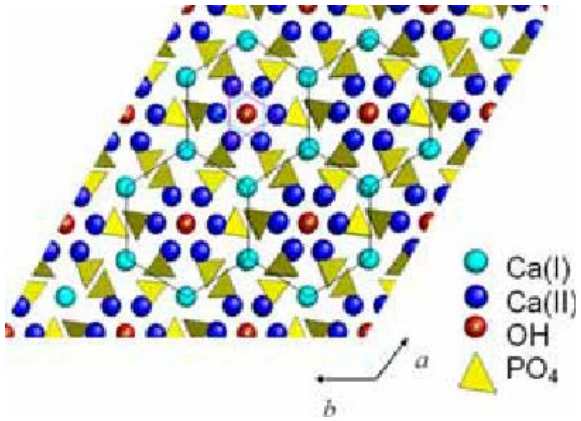

Figure 2. Hydroxyapatite structure along the c-axis[5]

HAp has important biomedical applications like dental implants, treatment of bone defects, fracture treatment, total joint replacement, craniomaxillofacial reconstructions, spinal surgery, and orthopaedics. It also has nonmedical and technological applications as a catalyst for chemical reactions such as the Michael-type

addition and methane oxidation, host materials for lasers, fluorescence materials, ion conductors and gas sensors.[2,7,12]

1.4. Applicability

This research is an investigation into alternative approaches for the titanium implants that do not normally bond to bone by producing a material that ideally will coat the implants and provide a strong suitable osseointegration implant.

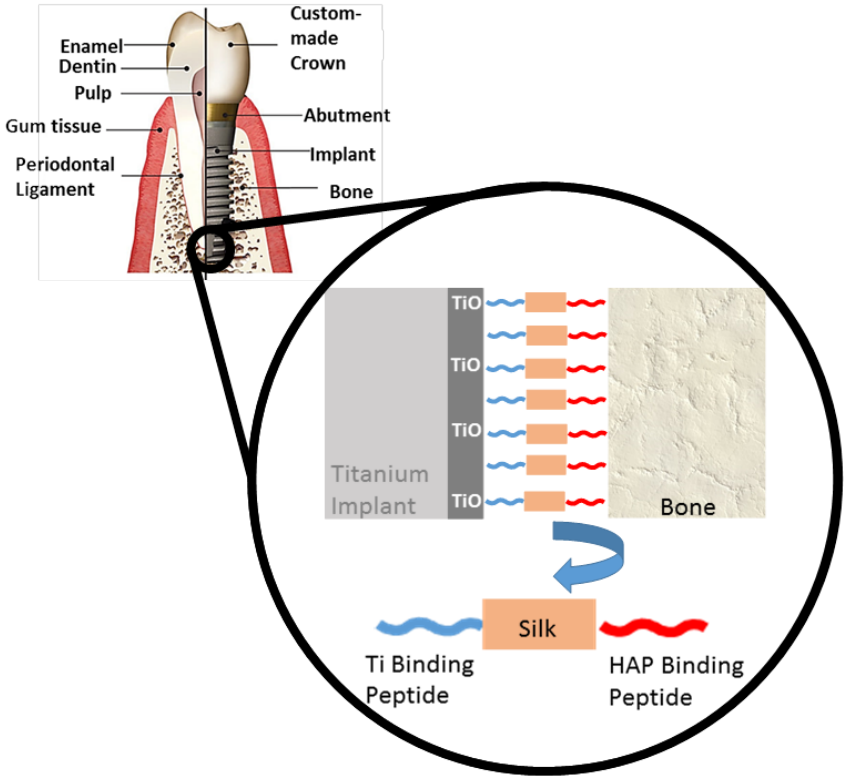

Figure 3. Dental implant focusing on structure of this research

Figure 3 shows a Dental implant's structure based on the current research, where every part of the proposed new implant is displayed. Spider silk materials are introduced because of the good physical proprieties, biocompatibility, and biodegradability. Knowing that silica has good compatibility with silk and biological systems, moreover, for the bioactivity with bone tissue, as it binds strongly with bone whilst also being osteoinductive. A combination of the best proprieties of silk and silica was found.[14]

To process and promote the silica deposition involves a set of proteins. The position of the protein R5 (SSKKSGSYSGSKGSKRRIL) has already been studied.[14] This current study tries to investigate the different effects of the peptides binding to HAp.

2. OBJECTIVES

The objective to be achieved in this study has been:

- Study the different effects of the peptides in the way of crystallising Calcium Phosphate. Look for the peptide that favours the crystalline route to Hydroxyapatite.

To reach this principal goal two sub-objectives were generated:

- Synthesise and characterize peptides. Including method development for characterization of these peptides by using:
  - Matrix Assisted Laser Desorption/Ionization Time of Flight Mass Spectrometry (MALDI-TOF).
  - High-performance liquid chromatography (HPLC).

- Growth of Hydroxyapatite in the presence of peptides by chemical methods, with characterization of the subtract formed using X-Ray Diffraction.

3. EXPERIMENTAL PART

3.1. Solvents and reagents

The following table summarizes the reagents and solvents of each experiment, additional information about each reagent and solvents can be found in *appendix 1*.

Table 3. Reagents and solvents used in the project

EXPERIMENT	REAGENTS	SOLVENTS
Peptide synthesis	- NMP - DEIA - HBTU - TFA - TIS - DODT - Amino Acids: Valine, Threonine, Lysine, Histidine, Leucine, Asparagine, Glutamine, Isoleucine, Serine, Tyrosine, Glycine, Methionine, Proline, Arginine, Alanine, Tryptophan, Glutamic Acid , Phenylalanine - Resin: Tyrosine, Proline, Threonine, Glutamic Acid	- DMF - DCM - Diethyl ether
Growth HAp	- $CaCl_2 \cdot 2H_2O$ - $Ca(NO_3)_2 \cdot 4H_2O$ - $(NH_4)_2HPO_4$ - Na_2HPO_4	- ddH_2O
MALDI-TOF		- ACN - ddH_2O - TFA
HPLC		- ACN - ddH_2O - TFA
Fluroscamine Assay	- Phosphate buffered saline (PBS) - Fluorescamine	

3.2. Synthesis and characterisation of peptides

3.2.1. Synthesis

Peptides are linear polymers made up of different combinations of amino acids, which are chemically linked together through an amide bond or peptide bond. [15]

To synthesise the peptides a Microwave Peptide Synthesizer was used for solid phase peptide synthesis (SPPS). This is a process by which chemical transformations can be carried out to a solid support (i.e. Merrifield resin) in order to prepare the desired peptides. This technique offers separation from soluble reagents by simple filtration and washing steps. However, by-products from incomplete couplings, side reactions, and impurities can build up on the solid supported together with the desired product.[16]

In the synthesis (*figure 4*) of peptides, the C-terminal amino acid is attached to a cross-linked polystyrene resin (the solid support) *via* an acid labile bond with a linker molecule. The resin is insoluble in the solvents used for synthesis (DMF), making it relatively simple and fast to wash away excess reagents and by-products. The N-terminus is protected with the Fmoc group, which is stable in acid, but removable by base. Any side chain functional groups are protected with base stable, acid labile groups.

To begin each coupling, the Fmoc group on the resin bound amino acid/peptide is removed with 20% piperazine in N,N-dimethyl formamide (DMF). It is then rinsed and the protected amino acid which has been activated at its “alpha” carboxyl group is added. The activation is achieved by creating the N-hydroxy-benzotriazole (HOBt) ester *in situ*. The activated amino acid (*aa*) and the resin bound *aa* are allowed to react in the presence of a base to form a new peptide bond. This process is repeated until the desired peptide is assembled at the resin.

Once the peptide is complete, it is ready to be cleaved from the resin.

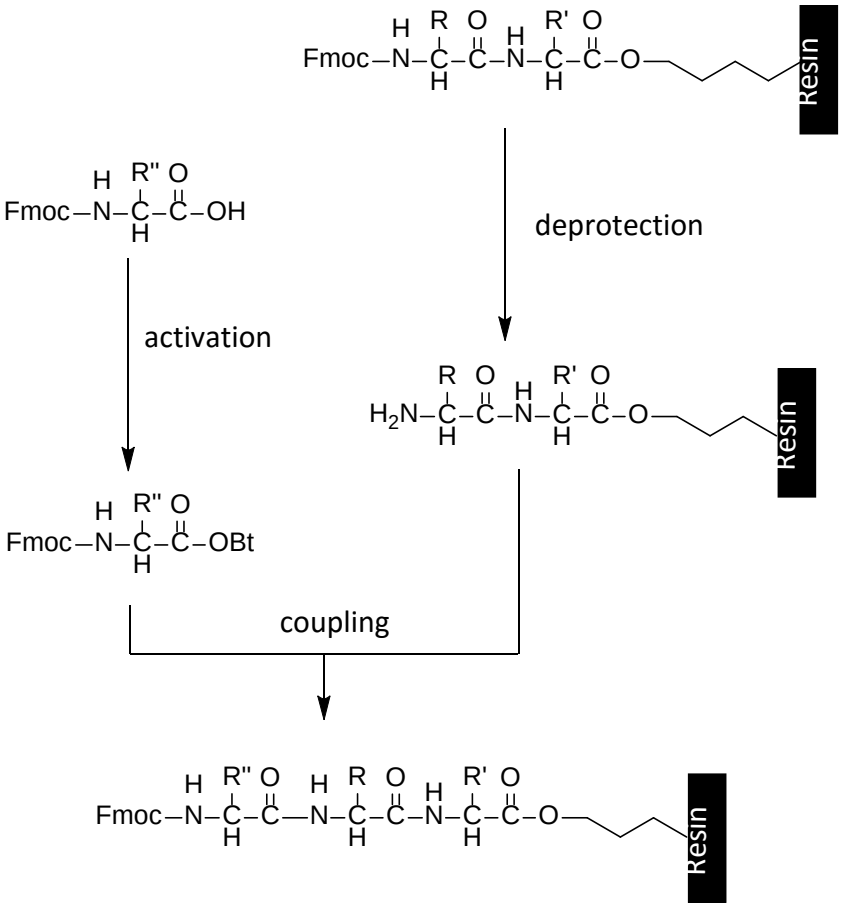

Figure 4. Scheme of the stepwise SPPS

Four peptides have been synthesised for the study of the crystallization and growth of Hydroxyapatite (calcium phosphate).

Table 4.Sequences of synthesised peptides.

Name	Sequence
CaP(V)	VTKHLNQISQSY
CaP(A)	APWHLSSQYSRT
CaP(S)	STLPIPHEFSRE
CaP(H)	SVSVGMKPSPRP

Microwave Peptide Synthesizer Standard Protocol:

1. **Clean system**. Depressurize of main wash, activator, activator base, all amino acids, and deprotector. Remove the bottles and change it for washing bottles, start the back flush and then back purge. Make sure, there is enough DMF.
2. **Preparation of solutions.** Extract reagents quantities vary depending on the target peptide, these are calculated based on the amino acids present by an

Exel file. It is also calculated the amount of activator (HBTU/DMF), activator base (DIEA/NMP), deprotector (Piperazine/DMF). All the solutions were sonicated thoroughly.

3. **Resin preparation.** Introduce the value mmole/g in the Exel file, and weight the amount calculated. Introduce it in the vessel previously cleaned by DMF.
4. **Place solutions in the system.** Depressurize all the bottles, and change the washing bottles for the bottles that contain required solution.
5. **Run method**. Search sequence of the peptide and start it. Wait 15 minutes to check everything is all right, then, synthesizing will start. It needs several hours, give it all night.
6. **Clean system** following the step number one.

Once the peptide is obtained it is necessary to cleave it from the resin. Prepare the cleavage solution in the fume cupboard:

Cleavage solution
- 0.25ml ddH_2O
- 0.1ml TIS
- 0.5ml DODT
- 9.4ml TFA

The resin-peptide was removed to one red-top tube, the cleavage solution was added and was stirred during two hours. After that time, 80-100ml of chilled diethyl ether was added in a bottle and the peptide precipitated. The stirred solution was removed in a vessel and it was connected to a pump. The peptide was finally collected into the diethyl ether bottle.

The peptide was washed with diethyl ether and separated by centrifugation. Centrifugation process: 4ºC at 5000rpm for 10 minutes. The pellet was separated from the supernatant and more chilled diethyl ether was added to the pellet. The cleaning process was repeated three times. Some holes were made in red-top and the diethyl ether evaporate fully before freeze-drying.

The sample was frozen in liquid nitrogen and lyophilized at -70ºC using a Viritis-110 freeze-dryer.

3.2.2. Techniques of characterisation

Peptide characterisation:

3.2.2.1. MALDI-TOF MS

MALDI-TOF MS (Matrix Assisted Laser Desorption/Ionization Time of Flight Mass Spectrometry).

This technique is based on four stages. The first, is ionization of the sample using laser irradiation, the ions are accelerated by an electric field and in the mass analyser (flight tube) dispersion according to the mass/charge ratio occurs. Finally, they are detected by the generate ion of an electric signal.[17]

The spectra of MALDI-TOF gives different information. One of the most important for characterising peptides is the base peak. This peak allows the main component to be assessed to determine if it is the expected peptide by verifying the ions molecular weight.

MALDI-TOF also indicates the purity of samples. A large number of peaks other than the molecular peak, means the sample has addition components or other amino acids in the peptide.

Moreover, by analysis of fragment ions. it is possible to check the order or sequence of the amino acids, to confirm that the synthesis has been carried out correctly.

Sample preparation. A solution of 50% of Acetonitrile (ACN), 50% ddH_2O and 0.1% of trifluoroacetic acid (TFA) was prepared. The minimum solution required is 250µl. A 1mg/ml peptide solution was then prepared for mass spectroscopy.

3.2.2.2. High-performance liquid chromatography

High-performance liquid chromatography (HPLC) is a technique that separates, identifies and quantifies the components according to the chemical and physical interactions between the column, the mobile phase, and the substance to analyse. The substance flows across the stationary phase (the column) with the help of the pump of the mobile phase. The degree of retention depends on nature of the compound and the composition of mobile phase and stationary phase. Here a C-18 column was used as it maximizes retention for moderately polar to non-polar compounds.[18]

The chromatogram allows checking and quantifying the purity of the peptide, thanks to the separation of the components. If it is pure, there is only one peak in the characteristic retention time of the peptide.

Sample preparation. A solution with 5% of Acetonitrile (ACN), 95% ddH_2O and 0.1% of trifluoroacetic acid (TFA) was prepared. 1mg of peptide was added to 1ml of HPLC solution.

3.3. Synthesis of Hydroxyapatite

HAp can be synthesized by different methods such as dry chemical methods by solid-state reactions, wet methods, and hydrothermal methods. *Figure 4* shows the sub-methods of the three main methods of HAp growth.

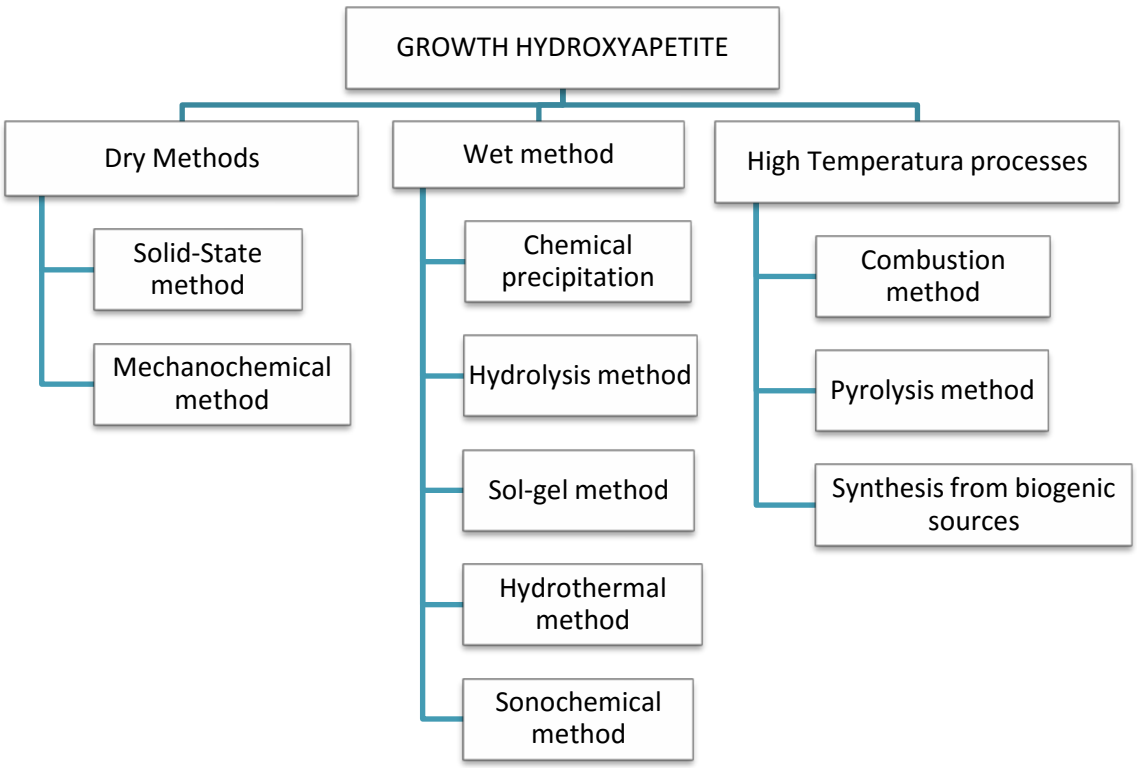

Figure 5.Outline of the different methods for preparation of Hydroxyapatite.[7]

The term "wet chemical methods" refers to a group of methods of powder and material production using the liquid phase at one of the process stages. It is characterized by the formation of small grains (crystallites) and short duration of phase formation.[19]

The advantages of growing HAp using wet chemical method are that it is easy to conduct and growth conditions can be directly controlled by adjusting the reaction parameters with ability to control the morphology and the mean size of the powder. The most important disadvantage is that at low temperature it generates other CaP phases (see *table 2*) and/or the lowering of the crystallinity of the resultant powder. Besides, the ions in aqueous solution can be incorporated in the crystal structure, causing trace impurities.[11]

The following equations show the chemical reactions with the reagents used in this work:[7]

$$10Ca(NO_3)_2 + 6(NH_4)_2HPO_4 + 8NH_4OH \rightarrow Ca_{10}(PO_4)_6(OH)_2 + 20NH_4NO_3 + 6H_2O$$

$10CaCl_2 + (NH_4)_2HPO_4 + 8NH_4OH \rightarrow Ca_{10}(PO_4)_6(OH)_2 + 20NH_4Cl + 6H_2O$

$10Ca(NO_3)_2 + 6Na_2HPO_4 + 2H_2O \rightarrow Ca_{10}(PO_4)_6(OH)_2 + 12NaNO_3 + 8HNO_3$

$10CaCl_2 + 6Na_2HPO_4 + 2H_2O \rightarrow Ca_{10}(PO_4)_6(OH)_2 + 12NaCl + 8HCl$

To avoid getting others phases, the best pH is around 11. Manoj, M. et al.[20] suggests that the formation of the HAp nanostructure was very weak when the pH values were 7 and 9 whereas increasing the pH value to 11.5 induced the formation of pure HAp. According to Swain, S. K. et al.[21] starting pH is an important parameter to optimize the morphology of HAp, and they start at pH 10. Studies byAngelescu, N. et al.[22]state in order to obtain a stoichiometric hydroxyapatite (Ca/P = 1.67) pH is increased 10.5. According to Koutsopoulos, S. et al.[23] It has been reported that at pH values above 10, formation of finely divided precipitates is favored so they worked at pH 9.5.

Because of the future biomedical applicability such as bone implant and treatment of this work, the reaction conditions chosed for this study has been 37ºC and physiological pH (7.4). This has been the biggest limitation for this study.

3.3.1. Methods of crystal growth

All the methods used in this work have been chemical precipitation. Two different methods have been employed:

METHOD 1.This method consists in mixing 50ml containing solution precursor of phosphate ions and 50ml of the solution precursor containing calcium ions.

As shown in *figure 5*, 12mM $(NH_4)_2HPO_4$ was added and the pH adjusted to 7.4 with HCl 1M. Next 1ml of a 1mg/ml aqueous peptide solution was added. It was placed in a shaking water bath to stabilize the solution at a temperature of 37ºC. Then with continuous stirring, $Ca(NO_3)_2$ solution was added dropwise. It was left for one hour to react.

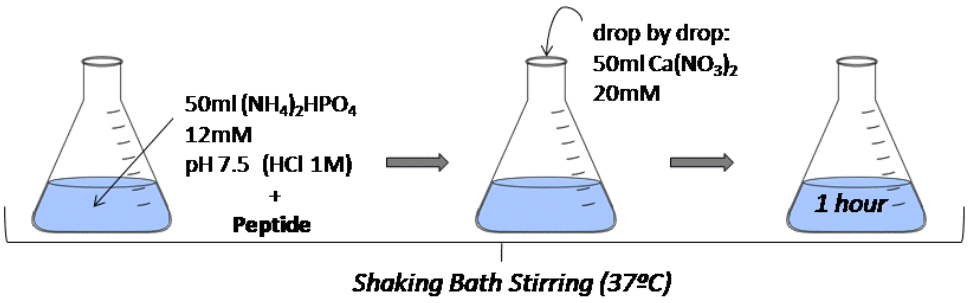

Figure 6. Drawing of growth HAp by method 1

The separation and cleaning process consisted of centrifugation (21ºC at 5000rpm for 7 minutes) and cleaning with distilled water to eliminate any soluble salts.

The samples were frozen in liquid nitrogen and lyophilized at -70ºC using a Viritis-110 freeze-dryer and to eliminate any volatile ammonium salts dried at 250ºC for one hour.

The method was developed for Caballeros-Alias, A. doctoral thesis[24] "*the role of silica in mineralising tissues"*. Some changes have been made regarding the original method. In the original method different molarities of orthosilicic acid were added to phosphate solution prior adjusting the pH to 7.4. The ionic strength was constant using NaCl as electrolyte. The time reaction was 30 min instead of 1 hour.

METHOD 2. Differs from method 1, in that small quantities of each solution were added sequentially until 2ml of each had been added.

In the shaking bath stirring at 37ºC, 1ml of a 1mg/ml aqueous peptide solution was added. Then 100µl of Na_2HPO_4 (120mM) solution was added and after one minute 100µl of the $CaCl_2$ (200mM) solution was added. This was repeated until adding a total of 2ml of each solution obtaining a total of 5ml. The reaction was then left to stir for one hour.

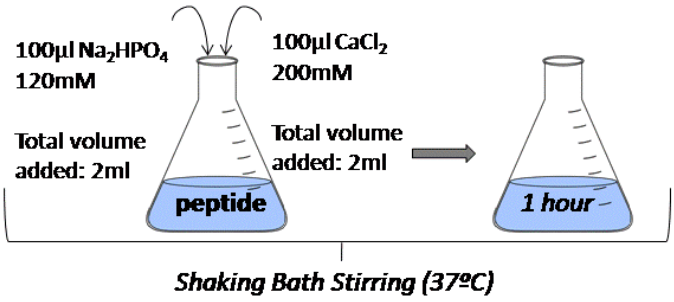

Figure 7. Drawing of growth HAp by method 2

To separate the precipitate from the solution centrifugation was used (21ºC at 5000rpm for 7 minutes) and to purify and clean the solid it was cleaned with distilled H_2O at least three times. The samples were frozen in liquid nitrogen and lyophilized at -70ºC using a Viritis-110 freeze-dryer.

Both methods were carried out using various reagents: calcium chloride ($CaCl_2 \cdot 2H_2O$), Calcium nitrate tetrahydrate ($Ca(NO_3)_2 \cdot 4H_2O$), di-ammonium hydrogen orthophosphate ($(NH_4)_2HPO_4$), sodium phosphate dibasic (Na_2HPO_4).

3.3.2. Technique of characterisation: X-Ray Diffraction

X-Ray Diffraction (XRD) is an important tool used to identify crystalline phases by comparison with data from known structures, quantify changes in the cell parameters, orientation, crystallite size and other structural parameters. It also allows identification the crystallographic structure of novel materials.

XRD is limited to crystalline materials, so it is difficult to apply this to solutions, biological systems, and it cannot be applied to amorphous or gaseous systems.

The X-Ray is electromagnetic waves of very short length, of the order of 0.1nm. The atomic space of solids is almost 0.1nm.

The X-Ray diffraction is based on the Bragg law. The sample is irradiated by X-Rays, when these rays reach an atom, they interact with the external electrons. These re-emit the incident electromagnetic radiation in different directions and with the same frequency. The re-emited rays interfere with each constructively or destructively. This is the phenomenon of diffraction.

The interference is constructive when the phase difference between the radiations emitted by different atoms is proportional to 2π. This condition is expressed in the Bragg law:

$$n\lambda = 2d \cdot sin(\theta)$$

- **n**, whole number
- **λ**, wavelength of X-rays,
- **d**, distance between the planes of the crystal lattice
- **θ**, angle between the incident rays and the planes of scattering

The spectrum data are compared with the International Centre for Diffraction Data (ICDD®), an organization dedicated to collecting, editing, publishing, and distributing powder diffraction data for the identification of materials.[25]

4. RESULTS AND DISCUSSIONS

4.1. Peptides

As discussed in *3.2.2.Techniques of characterization*, different techniques were used to identify and characterise each synthesised peptide.

4.1.1. MALDI-TOF results

Figure 8 shows the results of MALDI-TOF of each synthesised peptide.

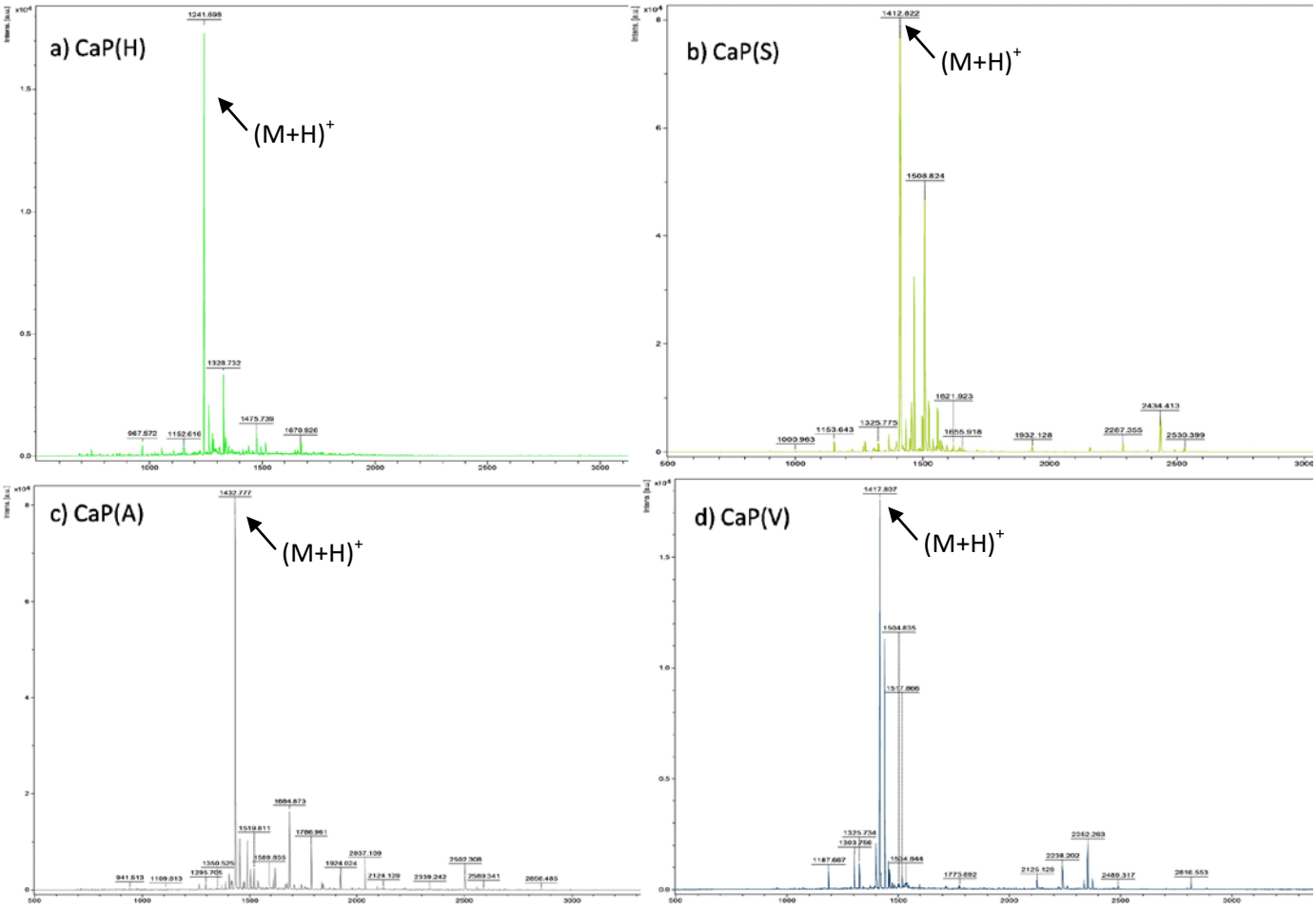

Figure 8.Spectra from MALDI-TOF analysis. a)CaP(H) b)Cap(S) c)CaP(A) d)CaP(V)

By comparing the peak base with the average weight of each peptide (see *table 5*) it was possible to confirm that each peptide had the correct mass.

Table 5. Comparison between base peak and average weight (g/mol)

	Base peak	Average Weight
CaP(H)	1241.698	1241.456 g/mol
CaP(S)	1412.822	1412.546 g/mol
CaP(A)	1432.777	1432.539 g/mol
CaP(V)	1417.807	1417.566 g/mol

Each peptide sample showed varying levels of impurities. The tables of *appendix2* show the identification of the main peak in each spectrum, and the possible impurities that the peptide samples contained.

By analysing the intensities of some of the peaks it was possible to highlight some impurities.

In CaP(H), the peak with the biggest relative intensity (20%) comparing with the peptide peak, corresponds to a weight loss of 88.083g/mol which can be identified as $(M+ACN+2Na+H)^+$. The ACN can come from the solution used to prepare the sample.

In CaP(S), there is a peak with a relative intensity of 60% that corresponds to a weight loss of 97.125g/mol. Due to the sequence being SVSVGMKPSPRP and the average mass of the amino acid Proline is 97.1167g/mol, everything indicates that same of the peptide made contained an extra amino acid.

In CaP(A)there was no remarkable peak, the component with the biggest relative intensity (20%) is from the cation $(M+Na)^+$.

Finally, CaP(V) there is a peak with a relative intensity of 60% in weight loss of 23.061g/mol this value is typical of the cation $(M+Na)^+$.

Once the molecular weight of each peptide is identified as correct, all other peaks were then considered in order to establish if each peptide has the correct amino acid order. The following tables show the verification of the peptide sequences.

Table 6. Sequence CaP(H)-SVSVGMKPSPRP

m/z	Intensity	Area	Amino Acid Mass	Amino Acid
115.164	5123.84	585	254.065	**PR** (Proline and Arginine)
369.229	48786.46	15421	87.034	**S** (Serine)
456.263	10853.97	3465	97.043	**P** (Proline)
553.306	62211.78	23397	128.097	**K** (Lysine)
681.403	19252.42	9005	131.062	**M** (Methionine)
812.465	9341.15	4842	57.013	**G** (Glycine)
869.478	14649.75	9055	186.042	**SV** (Serine and Valine)
1055.52	12929.94	7749	186.156	**SV** (Serine and Valine)
1241.676	37545.58	31125		Peak base

Table 7. Sequence CaP(S)-STLPIPHEFSRE

m/z	Intensity	Area	Amino Acid Mass	Amino Acid
304.006	7775.9	2658	86.998	**S** (Serine)
391.004	11884.42	3975	147.024	**F** (Phenylalanine)
538.028	50278.59	22138	129.026	**E** (GlutamicAcid)
667.054	23693.47	10933	137.068	**H** (Histidine)
804.122	11347.83	5201	97.053	**P**(Proline)
901.175	70243.99	46421	113.084	**I** (Isoleucine)
1014.294	7324.76	4381	97.101	**P** (Proline)
1111.395	33786.21	28690	113.13	**L** (Leucine)
1224.525	14138.18	12880	101.073	**T** (Threonine)
1325.598	6701.52	6630	87.205	**S** (Serine)
1412.803	29423.28	63125		Peak base

It was not possible to identify the last R (Arginine), it means that the resolution of the spectrum is not good enough. Or Arginine suffers another fragmentation as it has several functional groups that can be fragmented.

Table 8. Sequence CaP(V)-VTKHLNQISQSY

m/z	Intensity	Area	Amino Acid Mass	Amino Acid
180.91	433.34	14	87.069	**S**(Serine)
267.979	1445.15	110	215.899	**SQ** (Serine and Glutamine)
483.878	2137	470	605.362	**HLNQI** (Histidine, Leucine, Aspargine, Glutamine and Isoleucine)
1089.24	11849.91	11752	128.233	**K** (Lysine)
1217.473	5930.99	5259	200.299	**VT** (Valine and Threonine)
1417.772	5915.98	7868		Peak base

Table 9. Sequence CaP(A)-APWHLSSQYSRT

m/z	Intensity	Area	Amino Acid Mass	Amino Acid
275.9	1837.37	526	86.986	**S** (Serine)
362.886	3744.29	873	163.001	**Y** (Tyrosine)
525.887	5162.01	1606	128.039	**Q** (Glutamina)
653.926	6606.3	2686	87.007	**S** (Serine)
740.933	8150.78	3137	87.021	**S** (Serine)
827.954	6240.67	3441	113.119	**L** (Leucine)
941.073	4833.31	3321	491.665	**APWH** (Alanine, Proline, Tryptophan, and Histidine)
1432.738	5100.74	9777		Peak base

As before for CaP(S) it was not possible to observe the fragmentation of R (Arginine). It reaffirms the possibility of the different fragmentation of the amino acid.

4.1.2. HPLC results

To check the purity and quantify a high-performance liquid chromatography was performed on the samples.

Solvent A was water with 0.1% of acid trifluoroacetic (TFA) and solvent B was acetonitrile (ACN) with 0.1% of TFA. The purpose of TFA is to improve the separation of the peaks.

The method used for running was a flow of 0.5ml/min; a wavelength of 210nm; and a gradient as shown in *table 10*.

Table 10. Gradient used for HPLC

	0-1min	**1-20min**	**20-25min**	**25-30min**	**31-35min**
% solvent A	95%	30%	-	-	95%
% solvent B	5%	70%	100%	100%	5%

Because of peak splitting and broadening traces, this suggested that there were problems with the column. A control sample (*figure 9*), fluorescine, was run as a check and shown similar splitting, confirming the column issues.

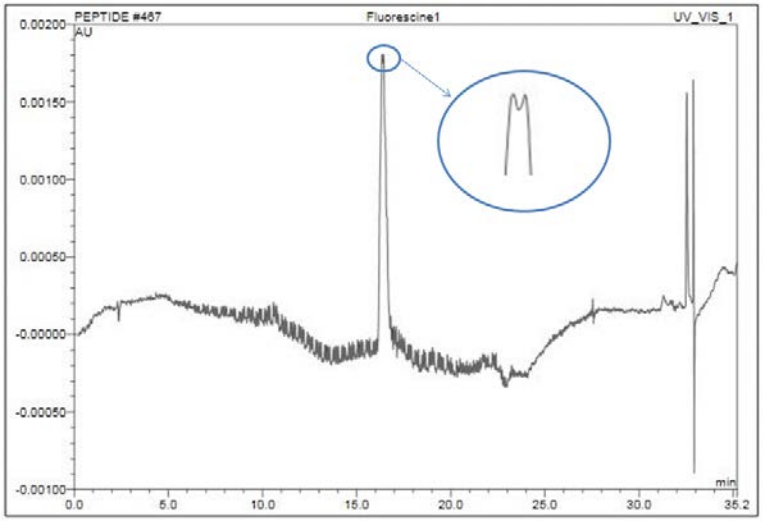

Figure 9. HPLC Fluorescine

The same method was used with another column, but the gradient of the solvents was not appropriate as the separation of the peaks was not clear enough. Therefore a change in gradient was used after trying several different ones, the optimum gradient was found, *table 11*.

Table 11. New gradient used for HPLC

	0-1min	**1-20min**	**20-25min**	**25-30min**	**31-35min**
% solvent A	95%	60%	-	-	95%
% solvent B	5%	40%	100%	100%	5%

The results are shown at *figure 10*.

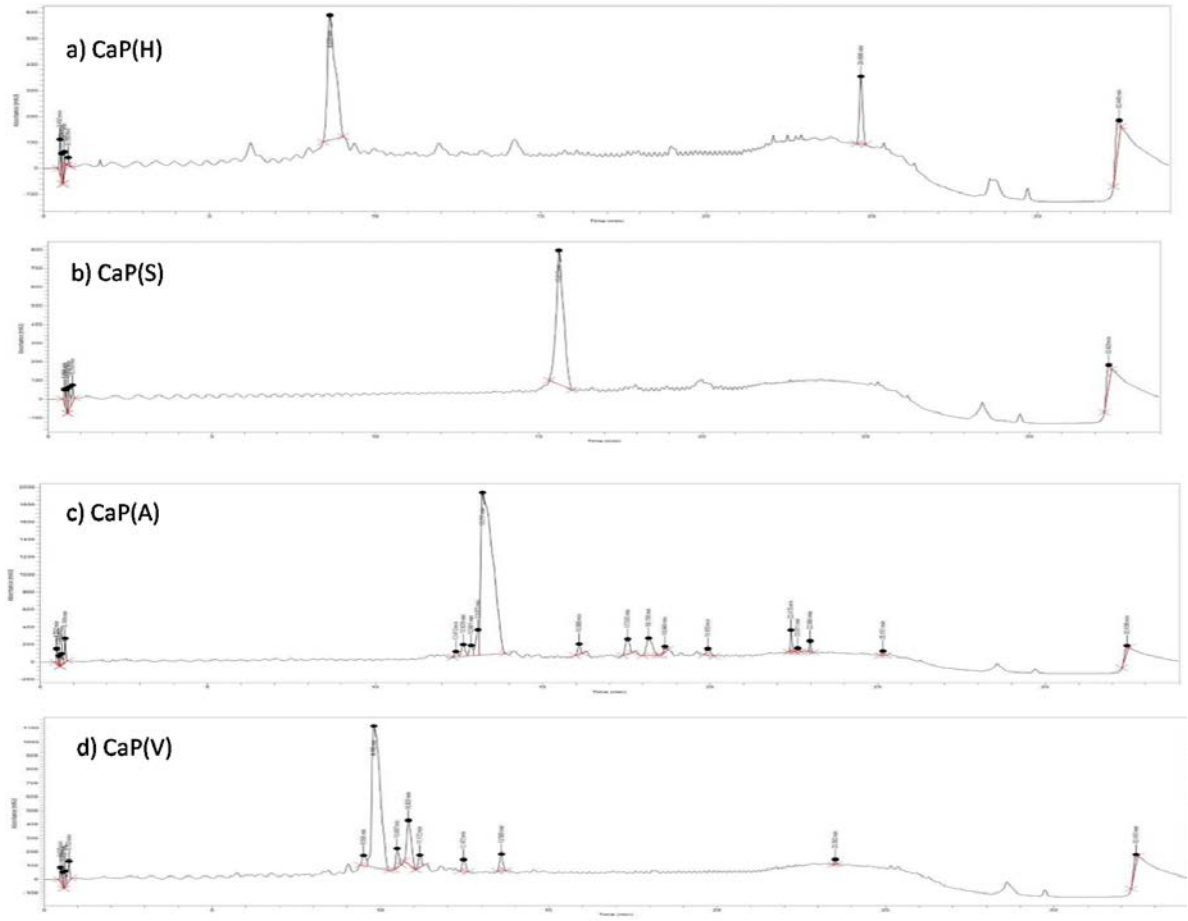

Figure 10. Chromatogram of HPLC. a)CaP(H) b)Cap(S) c)CaP(A) d)CaP(V)

In the following tables the peaks with each retention time and area are indicated.

Table 12. Peaks with retention time (RT) and their respective area

CaP(H)	RT (min)	8.639	24.666
	Area	8099696	1728806

CaP(S)	RT (min)	15.617
	Area	11316601

CaP(A)	RT(min)	12.413	12.626	12.861	13.076	13.211	16.086	17.535
	Area	446526	1048864	897327	2004201	45636384	739477	1545702
	RT(min)	18.156	18.649	19.933	22.415	22.611	22.984	25.151
	Area	2482096	367841	677741	794400	263172	386874	190486

CaP(V)	RT(min)	9.506	9.795	10.497	10.826
	Area	610041	17413528	865868	3003846
	RT(min)	11.172	12.472	13.589	23.502
	Area	589032	625689	812968	37646

With the results of HPLC was possible to calculate the purity of each peptide (*table 13)*.

Table13.Purity of peptides

	CaP(H)	CaP(S)	CaP(A)	CaP(V)
Purity (%)	82.4%	≅100%	79.4%	72.7%

4.1.3. ^{1}H NMR results

Because of the level of fragmentation that was observed in the mass spectra and the various complications due to the column in HPLC, it was decided to perform ^{1}H NMR on the samples. The ^{1}H NMR spectra were compared to spectra of purchased peptides, to see any differences between them.

The solvent used was deuterated dimethylsulfoxide$(CD_3)_2SO$.

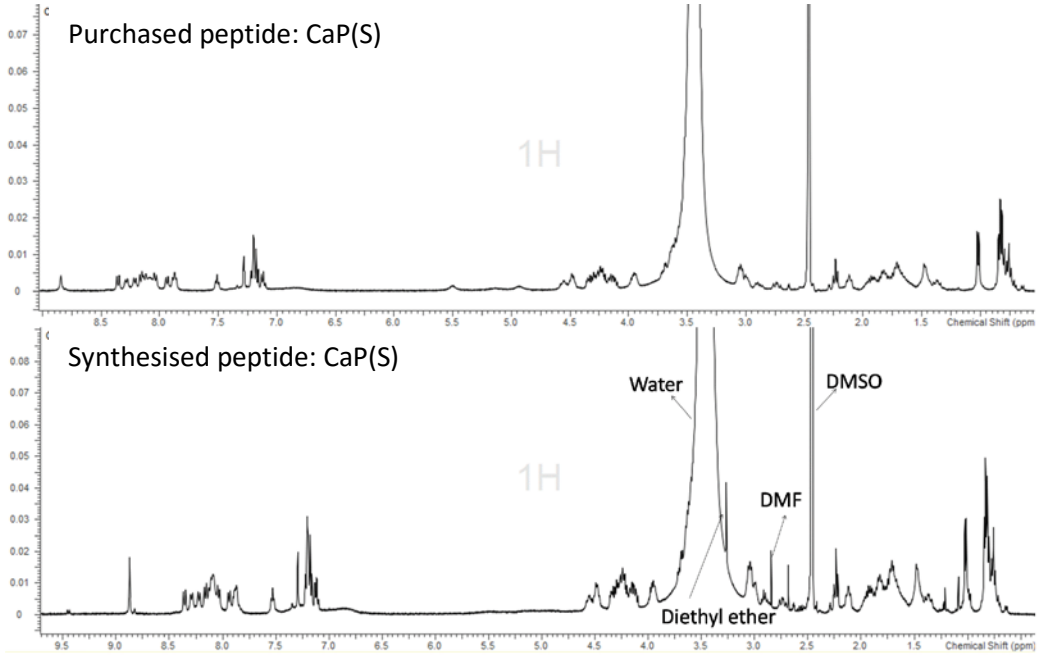

Figure 11. Comparison of ^{1}H NMR spectra of CaP(S)-STLPIPHEFSRE

Comparing the two spectra it was possible to identify some peaks from solvents used: the protons of the CH_3 from DMF appeared at around 2.89ppm.[26] The CH_2 protons of diethyl ether appeared at 3.38ppm.[26]

The other peaks of the spectrum are quite similar and have the same multiplicity. It means that CaP(S) is good enough for working with. Although, there is the peak at 9.4ppm that was not possible to identify and the ones at 8.9ppm that indicate that there is an impurity.

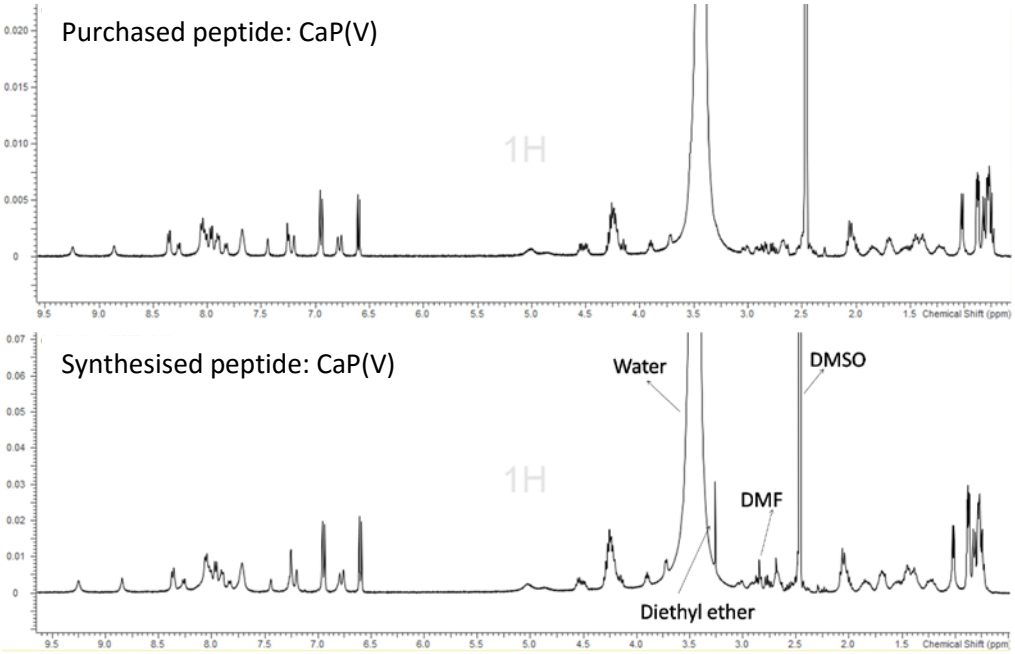

Figure 12. Comparison of ^{1}H NMR spectra of CaP(V)

These spectra are very similar. All peak positions agree and also the multiplicity of each peak are the same. It is also possible see the peaks of solvents, DMF (2.89ppm[26]) and diethyl ether (3.38ppm[26]).

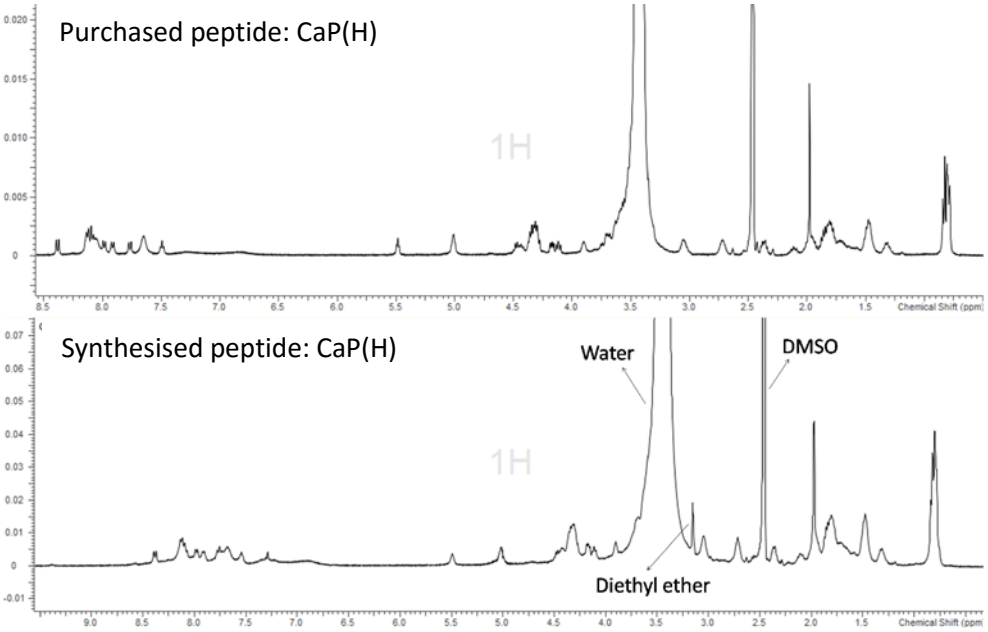

Figure 13. Comparison of ^{1}H NMR spectra of CaP(H)

These spectra (*figure 13)* are the ones that have less similarity in the multiplicity of the peaks in the zone 7-8.5 ppm. Despite these results, which are probably mainly due to loss of resolution and considering the results of HPLC and MALDI-TOF confirm that the project can be carried out with these peptides. The lost of the multiplicity is most likely loss of resolution due to impurities and particulates.

4.2. Hydroxyapatite

The crystalline nature prepared in the two different methods was analysed using X-Ray diffraction (XRD). Successfull and reproducible results with *method 1* were achieved by using the peptides CaP(S), CaP(V), and CaP(A). *Method 2* did not succesfuly produce the target mineral (HAp), but a complete study of the adsorption of each peptide in the solid was carried out by Fluorescamine Assay.

4.2.1. Results method 1

To study the reagent influences obtaining the crystallization of solid, different samples without presence of peptide (blanks) were prepared with all the possible combinations of reagents shown in *table 15*.

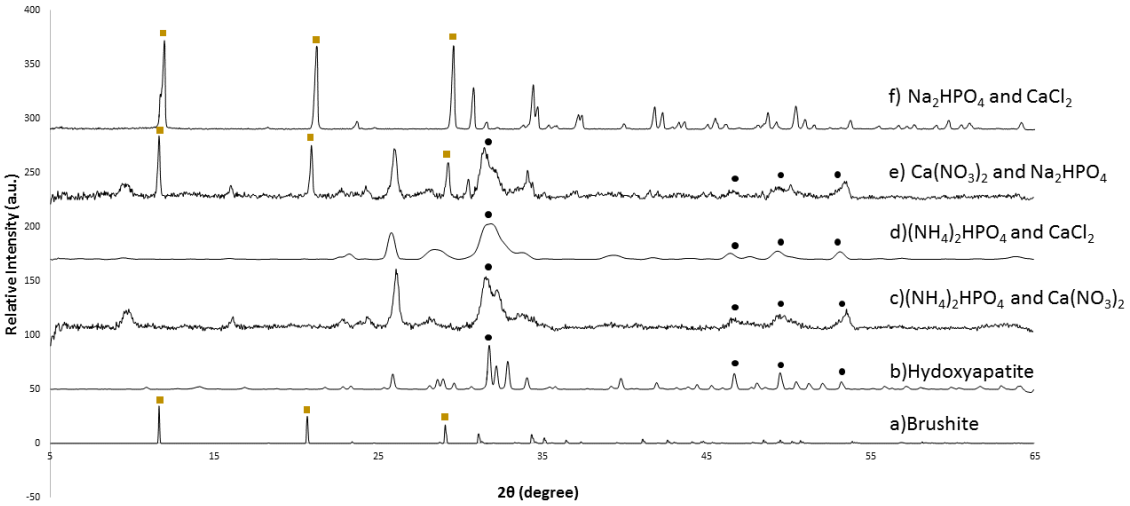

Figure 14. XRD data of differents blanks (37ºC and pH 7.4) a)Brushite Pattern b)Hydroxyapatite Pattern c)(NH4)2HPO4/Ca(NO3)2 reagents d)(NH4)2HPO4/CaCl2 reagents e)Ca(NO3)2/Na2HPO4 reagents f)Na2HPO4/CaCl2 reagents

Table 14. Summary of the reagents and the results obtained.

$(NH_4)_2HPO_4$	$Ca(NO_3)_2$	Na_2HPO_4	$CaCl_2$	Result
X	X	-	-	HAp
X	-	-	X	HAp
-	X	X	-	HAp/Brushite
-	-	X	X	Brushite

Blanks were prepared under the same conditions of pH 7.4 and 37ºC. Each reaction was used with the same volumes (50ml) of calcium (Ca^{2+}) and phosphate (HPO_4^{2-}) precursors.

These results demonstrate that the reagents chosen are important factors for the growth of the mineral HAp. There are studies that suggested that previous phases, like Brushite, were identified during HAp formation in solution[27]. That could explain the presence of this phase in the results. $(NH_4)_2HPO_4/Ca(NO_3)_2$ and $(NH_4)_2HPO_4/CaCl_2$ diffactogram show the presence of just HAp, so these reagents including the formed salts, favour the complete conversion. Using $Na_2HPO_4/Ca(NO_3)_2$ two phases are presents, HAp and Brushite, so in solutions containing these reagents the Brushite phase could be the epitaxial nucleator for HAp. And $Na_2HPO_4/CaCl_2$ would be the reagents that less favoured the transformation of the epiaxial nucleation, for this reason just Brushite phase was identified by XRD.

The complete study of *method 1* using each synthesised peptide , was carried out with the reagents of original method$(NH_4)_2HPO_4$and $Ca(NO_3)_2$, to see how the peptides affect the growth process.

Figure 15 shows the XRD results from *method 1* before the last step of heating the samples at 250ºC during 1 hour, using $(NH_4)_2HPO_4$ (12mM) and $Ca(NO_3)_2$ (20mM).

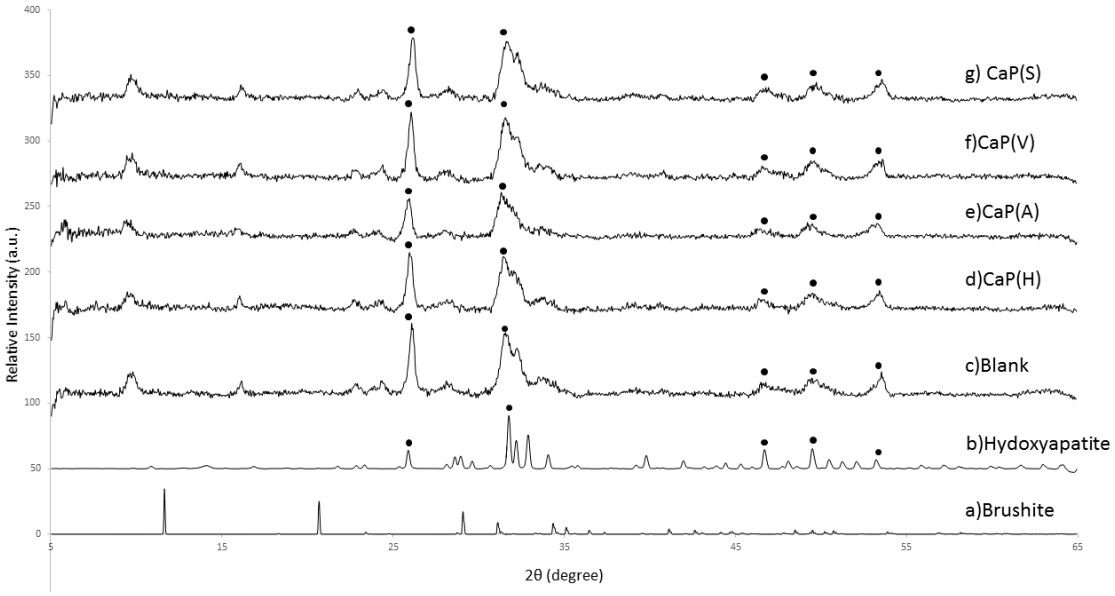

Figure 15. XRD data before heating: a)Brushita pattern b)Hydroxyapatite pattern c)Blank d)Calcium phosphate containing CaP(H)-SVSVGMKPSPRP e)Calcium phosphate containing CaP(A)-APWHLSSQYSRT f)Calcium phosphate containing CaP(V)-VTKHLNQISQSY g)Calcium phosphate containing CaP(S)-STLPIPHEFSRE

The diffractogram *a)* corresponds to Brushite pattern and *b)* to Hydroxyapatite pattern.

Studying the data of XRD of the growth of calcium phosphate by *method 1* using $(NH_4)_2HPO_4$ and $Ca(NO_3)\cdot 4H_2O$ before heating, in all samples characteristic HAp peaks were identified, see in *table 15*, obtaining the target product.

Regarding to crystallinity of the samples that contain peptide, CaP(S) is the one with better definition of the peaks, followed by CaP(V) and CaP(H).

Table 15. Matching peaks between HAp pattern and the samples containing peptide

2θ (degree)	(hkl) plane	d (Å)
25.879	(002)	3.44000
31.739	(211)	2.81700
39.765	(130)	2.26500
46.662	(222)	1.94500
49.463	(213)	1.84120

After the complete treatment of heating during 1hour at 250ºC, the results are shown in *figure 16*.

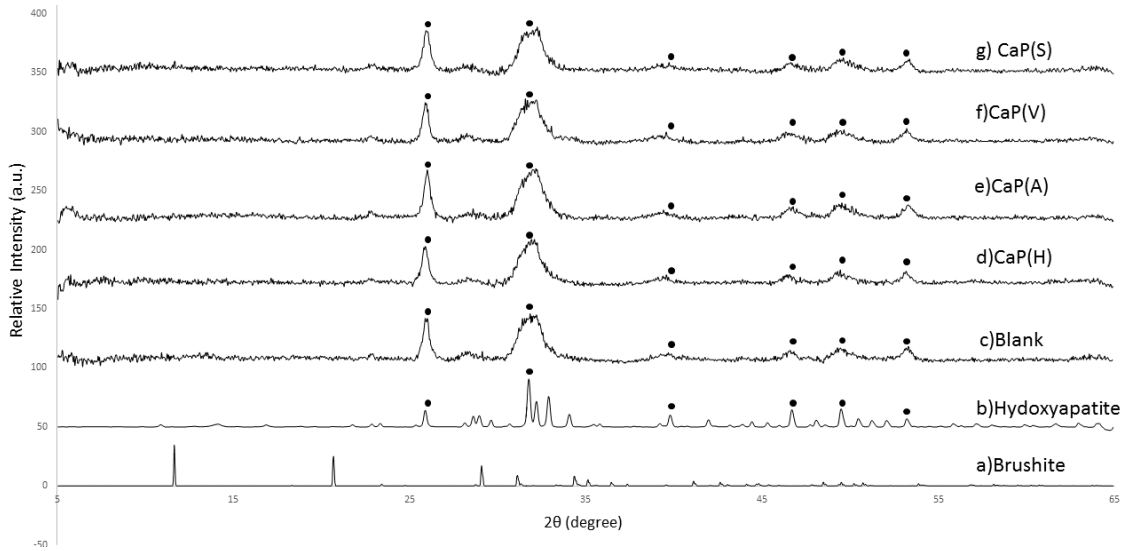

Figure 16. XRD data after heating (1h. 250ºC): a)Brushite pattern b)Hydroxyapatite patern c)Blank d)Calcium phosphate containing CaP(H)-SVSVGMKPSPRP e)Calcium phosphate containing CaP(A)-APWHLSSQYSRT f)Calcium phosphate containing CaP(V)-VTKHLNQISQSY g)Calcium phosphate containing CaP(S)-STLPIPHEFSRE

Some differences in the first part of the diffractogram were observed, getting more clean results which means that all volatile ammonium salts where eliminated for temperature treatment. And a peak at 39.765 degrees corresponding to the (130) plane was then able to be observed.

The method was repeated several times to have consistent data and results. CaP(A), CaP(V) and CaP(S) agree in all of the repetitions, nevertheless for Blank and CaP(H) samples, as possible to see in *figure 16*, in some repeat samples it was possible to identify Brushite peaks.

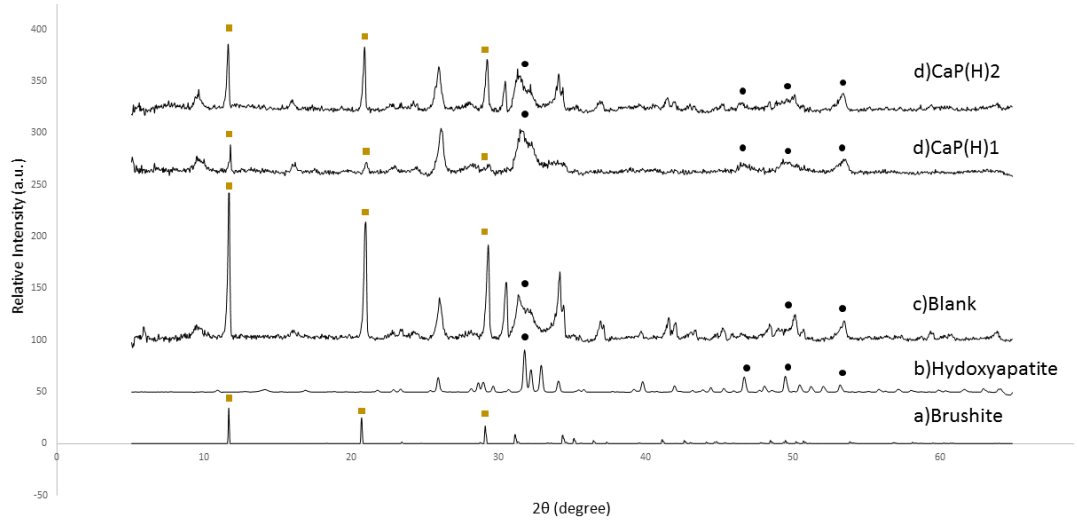

Figure 17. Results of some repeated of method 1 before heating a)Brushite Pattern b)Hydroxyapatite Pattern c)Blank d)CaP(H) repetition 1 d) CaP(H) repetition 2

Thus, obtaining HAp without other phases present in the structure by using the peptide CaP(H) and without the use of any peptide was not completely reliable.

The samples were heated during 1hour at 250°C, and the results were (*figure 17*):

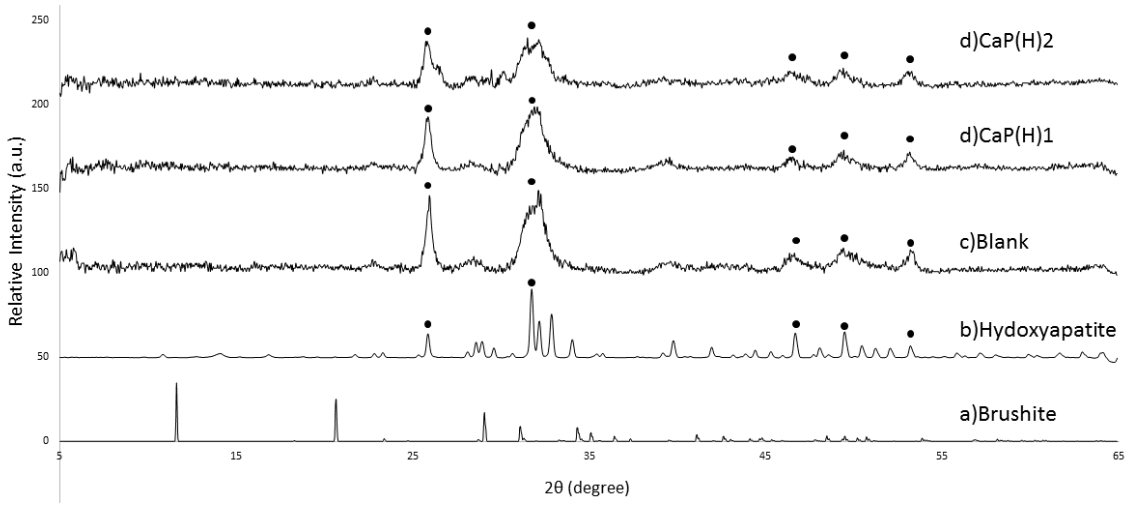

Figure 18. XRD data of some repeated of method 1 after heating (1h. 250ºC) a)Brushite Pattern b)Hydroxyapatite Pattern c)Blank d)CaP(H) repetition 1 d) CaP(H) repetition 2

The samples after heating coincide with the structure of the samples after heating in *figure 15*.The most important observation between the before and after the heating was that the samples before heating were a mix of Brushite and HAp, after heating only HAp was identified. The crystals reorganise into the more stable HAp. It was also shown that ammonium salts has been removed.

Most blanks already produce HAp, thus obtaining the target compound of the study. This would generate the advantage of lower the price of the target compound, but for the applicability for the new type of implant explained in section *1.4.Applicability* is

important the presence of peptides for the connection of all parts. So with the results it was possible to conclude that utilization of *method 1* with presence of CaP(V), CaP(A) and CaP(S) Hydoxyapatite were always favoured.

4.2.2. Results method 2

Figure 16 shows the results from *method 2*, using Na_2HPO_4 (120mM) and $CaCl_2$ (200mM).

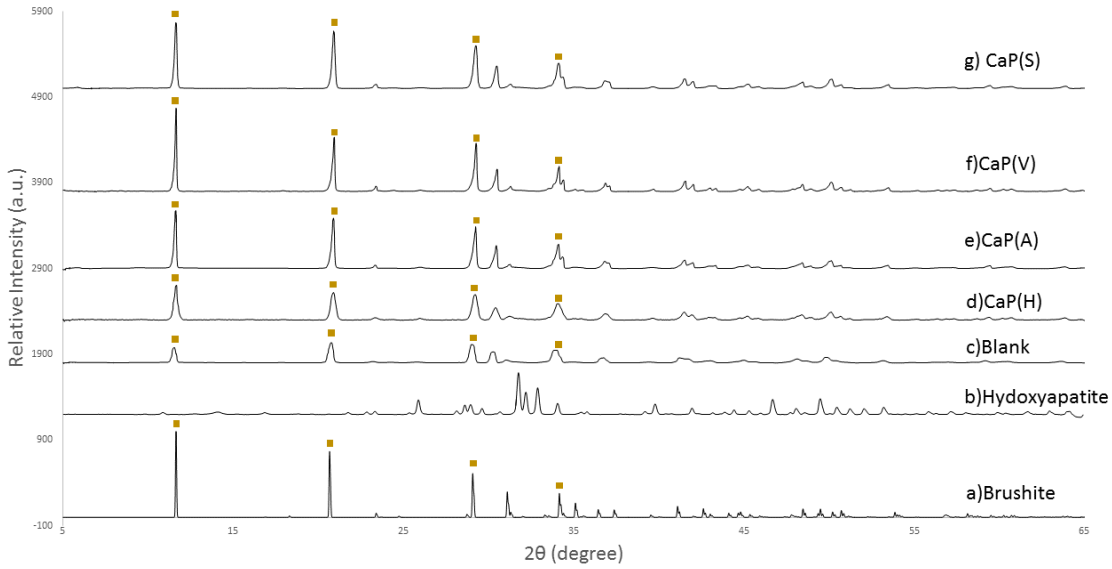

Figure 19. XRD data method 2. a)Brushite pattern b) Hydroxyapatite pattern c)Blank d)calcium phosphate containing CaP(H)-SVSVGMKPSPRP e)calcium phosphate containing CaP(A)-APWHLSSQYSRT f)calcium phosphate containing CaP(V)-VTKHLNQISQSY g)calcium phosphate containing CaP(S)-STLPIPHEFSRE

Regarding to this method it was possible to identify only the Brushite phase. In *table16* is identified the peaks with the each corresponding value of 2 theta degree and planes that verify the Brushite phase.

Peaks at 29.160º and 35.452º in CaP(V), CaP(A), and CaP(S) have better crystallinity with more narrow and defined peaks than CaP(H) and Blank.

Table 16.Matching peaks between Brushite pattern and the synthesised samples

2θ	(hkl) plane	d (Å)
11.604	(020)	7.62000
23.391	(040)	3.80000
29.160	$(\bar{1}12)$	3.06000
35.452	$(\bar{2}31)$	2.53000

Obtaining only Brushite creates the question if there was any interaction between the peptide and the calcium phosphate. If there had been some interaction his would mean that the presence of the peptide was not affecting the morphology, otherwise, if there had not been any interaction this would explain the obtaining of Brushite in all of them. For checking it, a Fluorescamine Assay was carried on. The Flourescamine reacts (*figure 20*) with the primary amino groups forming fluorescent moieties.[28] The first supernatant of the separation between the solid and the precipitate was quantified, getting positive results shown in *table 17*.

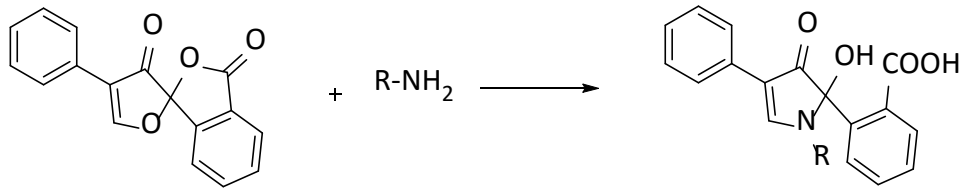

Fluorescamine

Figure 20. Reaction between Fluorescamine and primary amino group

Table 17. Results of Fluorescamine Assay

	Maximum [peptide]	**[peptide] in supernatant**	**[peptide] in solid**	**% adsorption in solid**
CaP(A)	0.312	0.057	0.254	**81.5%**
CaP(H)	0.272	0.088	0.183	**67.5%**
CaP(S)	0.316	0.146	0.169	**53.7%**
CaP(V)	0.250	0.008	0.241	**96.6%**

Knowing that there was an interaction between the peptide and the CaP and observing the results of XRD it was possible to confirm that *method 2* was not working properly and the peptides were binding but without influence on the crystallography of the material produced.

5. CONCLUSIONS

The goal of this project was to study the different effects of the peptides (CaP(H)-SVSVGMKPSPRP CaP(V)-VTKHLNQISQSY CaP(S)-STLPIPHEFSRE and CaP(A)-APWHLSSQYSRT) on the crystallisation of the calcium phosphate to find out which is the one that favours formation the HAp phase.

To achieve this main goal, it was necessary to complete two sub-objectives. One was the synthesis and characterisation of the peptides which was successfully done, so the work was carried on with the four peptides synthesised.

The other goal, was finding a wet chemical method that allows the HAp phase to form. Two methods were tested and in only *method 1* HAp phase was obtained.

In the study of the different effects of each peptide the results were too similar for verifying some favouritism for one peptide. Nevertheless, due to repeating the method it is possible to confirm that CaP(V), CaP(S), and CaP(A) always give HAp meanwhile CaP(H) in not as reliable for getting HAp.

6. REFERENCES

(1) Nottingham Trent University. http://www.ntu.ac.uk/apps/staff_profiles/staff_directory/125634-2/26/carole_perry.aspx (accessed May 2, 2016).

(2) Dorozhkin, S. Bioceramics of Calcium Orthophosphates. *Biomaterials* **2010**, *31* (7), 1465–1485.

(3) MORALEDA, B. F.-M. Optimización de Materiales Para Regeneración Ósea . Estudio de Las Interacciones de Hidroxiapatita Con Proteínas Y Preparación de Andamios Porosos, **2013**.

(4) Pérez Llamas, Francisca, Garaulet Aza, Marta; Gil Hernández, Ángel; Zamora Navarro, S. Calcio, Fosforo, Magnesio Y Fluor. Metabolisom Óseo Y Su Regulación. In *Tratado de Nutrición Tomo I*; **2005**; pp 897–926.

(5) Roy, M. D.; Stanley, S. K.; Amis, E. J.; Becker, M. L. Identification of a Highly Specific Hydroxyapatite-Binding Peptide Using Phage Display. *Adv. Mater.* **2008**, *20* (10), 1830–1836.

(6) Weiger, M. C.; Park, J. J.; Roy, M. D.; Stafford, C. M.; Karim, A.; Becker, M. L. Quantification of the Binding Affinity of a Specific Hydroxyapatite Binding Peptide. *Biomaterials* **2010**, *31* (11), 2955–2963.

(7) Sadat-Shojai, M.; Khorasani, M. T.; Dinpanah-Khoshdargi, E.; Jamshidi, A. Synthesis Methods for Nanosized Hydroxyapatite with Diverse Structures. *Acta Biomater.* **2013**, *9* (8), 7591–7621.

(8) Campbell, J. NIH Public Access. **2011**, *1* (2), 93–106.

(9) Camera, D. S. *Instruction Manual*; **2008**; Vol. 11.

(10) Segvich, S.; Biswas, S.; Becker, U.; Kohn, D. H. Identification of Peptides with Targeted Adhesion to Bone-like Mineral via Phage Display and Computational Modeling. *Cells Tissues Organs* **2008**, *189* (1-4), 245–251.

(11) Segvich, S. J.; Smith, H. C.; Kohn, D. H. The Adsorption of Preferential Binding Peptides to Apatite-Based Materials. *Biomaterials* **2009**, *30* (7), 1287–1298.

(12) Krishnamurithy, G. A Review on Hydroxyapatite-Based Scaffolds as a Potential Bone Graft Substitute for Bone Tissue Engineering Applications. *J. Univ. Malaya Med. Cent.* **2013**, *16* (2), 1–6.

(13) Xia, W.; Lindahl, C.; Lausmaa, J.; Engqvist, H. *Biomimetic Hydroxyapatite Deposition on Titanium Oxide Surfaces for Biomedical Application*; **2011**.

(14) Plowright, R.; Dinjaski, N.; Zhou, S.; Belton, D. J.; Kaplan, D. L.; Perry, C. C. HHS Public Access. **2016**, *6* (26), 21776–21788.

(15) Hoffmann, E. de.; Stroobant, V. *Mass Spectrometry : Principles and Applications*; J. Wiley, **2007**.

(16) CEM Company. Microwave Peptide Synthesis http://www.cem.com/peptide-synthesis.html (accessed Apr 20, 2016).

(17) Universidad de Valencia. Fundamentos y funciones de la espetrometria de masas http://mural.uv.es/caloan/#Palabras_clave (accessed Apr 12, 2016).

(18) Technologies, A. Guía de selección de columnas Agilent ZORBAX para HPLC http://www.analitica.cl/PDF/INSUMOS/Columnas HPLC.pdf (accessed Apr 19, 2016).

(19) Rusnano. Glossary of nano technology and relate terms http://eng.thesaurus.rusnano.com/wiki/article1209 (accessed Apr 28, 2016).

(20) Manoj, M.; Subbiah, R.; Mangalaraj, D.; Ponpandian, N.; Viswanathan, C.; Park, K. Influence of Growth Parameters on the Formation of Hydroxyapatite (HAp) Nanostructures and Their Cell Viability Studies. *Nanobiomedicine* **2015**, 1.

(21) Swain, S. K.; Sarkar, D. A Comparative Study: Hydroxyapatite Spherical Nanopowders and Elongated Nanorods. *Ceram. Int.* **2011**, *37* (7), 2927–2930.

(22) Angelescu, N.; Ungureanu, D. N.; Anghelina, F. V. Synthesis and Characterization of Hydroxyapatite. **2011**, *6* (6), 15–18.

(23) Koutsopoulos, S. Synthesis and Characterization of Hydroxyapatite Crystals : A Review Study on the Analytical Methods. **2002**, No. February, 31–34.

(24) Caballero-Alias, A. The Roles of Silica in Mineralizing Tissues, Nottingham Trent University, **1999**.

(25) ICDD. The International Centre for Diffraction Data http://www.icdd.com/profile/index.htm (accessed May 7, 2016).

(26) Fulmer, G. R.; Miller, A. J. M.; Sherden, N. H.; Gottlieb, H. E.; Nudelman, A.; Stoltz, B. M.; Bercaw, J. E.; Goldberg, K. I. NMR Chemical Shifts of Trace Impurities: Common Laboratory Solvents, Organics, and Gases in Deuterated Solvents Relevant to the Organometallic Chemist. *Organometallics* **2010**, *29* (9), 2176–2179.

(27) B.E.C.Nordin. *Calcium in Human Biology*, 1st ed.; Springer-Verlag: Berlin, **1988**.

(28) Held, P. G. Fluorometric Quantitation of Protein Using the Reactive Compound Fluorescamine. **2006**.

APPENDIX

Appendix 1. Information list of solvents and reagents used

SOLVENTS

- N,N-Dimethylformamide (DMF), extra pure. Fisher
- Dichloromethane (DCM), 99%. Fisher
- Diethyl ether, extra pure. Fisher
- Acetonitrile (ACN), ≥99,9%. Sigma-Aldrich
- Water (H_2O). Sigma-Aldrich

REAGENT

- Thioanisol (TIS). Sigma-Aldrich
- 1-methil-2-pyrrolidone (NMP). Rathburn Chemicals
- N,N-Diisopropyl-ethylamina (DIEIA). AGTC Bioproducts
- Trifluoroacetic acid (TFA), 99%. Sigma-Aldrich
- 2,2'-(Ethylenedioxy)diethanethiol (DODT), 95%. Sigma-Aldrich
- Piperazine, 99%. Sigma-Aldrich
- 2-(1H-Benzotriazole-1-yl)-1,1,3,3-tetramethyluronium hexafluorphosphate (HBTU). AGTCBioproducts
- Di-ammonium hydrogen orthophosphate, ≥97%. British drug house
- Sodium phosphate dibasic, ≥98%. Sigma-Aldrich
- Calcium Chloride. Sigma-Aldrich
- Calcium nitrate tetrahydrate, ≥99%. Sigma-Aldrich
- Phosphate buffered saline (PBS) tablets. Fisher
- Fluorescamine, ≥98%. Sigma-Aldrich
- Valine (V).NovabiochemFmoc-Val-OH. Merk
- Threonine (T). NovabiochemFmoc-Thr(tBu)-OH. Merk
- Lysine (K). NovabiochemFmoc-Lys(Boc)-OH. Merk
- Histidine (H). NovabiochemFmoc-His(Trt)-OH. Merk
- Leucine (L). NovabiochemFmoc-Leu-OH. Merk
- Asparagine (N). NovabiochemFmoc-Asn-OH. Merk
- Glutamine (Q). NovabiochemFmoc-Gln(Trt)-OH. Merk
- Isoleucine (I). NovabiochemFmoc-Ile-OH. Merk
- Serine (S). NovabiochemFmoc-Ser(tBu)-OH. Merk
- Tyrosine (Y). Fmoc-Tyr(tBu)-OH. CEM
- Glycine (G). NovabiochemFmoc-Gly-OH. Merk
- Methionine (M). NovabiochemFmoc-Met-OH. Merk

- Proline (P). NovabiochemFmoc-Pro-OH. Merk
- Arginine (R). NovabiochemFmoc-Arg(Pbf)-OH. Merk
- Alanine (A). NovabiochemFmoc-Ala-OH. Merk
- Tryptophan (W). NovabiochemFmoc-Trp(Boc)-OH. Merk
- Glutamic Acid (E). NovabiochemFmoc-Glu(OtBu)-OH. Merk
- Phenylalanine (F). NovabiochemFmoc-Phe-OH. Merk
- Tyrosine (Y) Resin. NovabiochemFmoc-Tyr(tBu)-wangresin (100-200 mesh). Merk
- Proline (P) Resin. NovabiochemFmoc-Pro-NovaSyn TGT. Merk
- Threonine (T) Resin. Fmoc-Thr(tBu)-wang resin (100-200 mesh). Novabiochem
- GlutamicAcid (E) Resin. NovabiochemFmoc-Glu(OtBu)-wangresin (100-200 mesh). Merk

Appendix 2. Informative table with possible impurities of each peptide identified by MALDI-TOF

Table a. Identification of the main picks of CaP(H) of MALDI-TOF

S/N	Intensity	Area	Weight lost (m/z-mass)	Identification
665.4	17566.29	3744	1.049	$(M+H)^+$
76	2050.52	392	23.032	$(M+Na)^+$
30.1	830.19	181	39.01	$(M+K)^+$
14.6	413.29	76	43.019	
123.1	3427.27	672	88.083	$(M+ACN+2Na+H)^+$
22.5	641.6	166	97.041	
21	603.76	175	100.045	
11	324.66	75	110.062	
34.9	1021.77	238	235.09	
17	499.48	139	275.124	
18.1	501.01	128	430.277	molecular peak

Table b. Identification of the main picks of CaP(S) of MALDI-TOF

S/N	Intensity	Area	Weight lost (m/z-mass)	Identification
1412.822	76395.67	68276	1.123	$(M+H)^+$
1414.854	17472.2	6120	3.155	
1422.921	910.99	706	11.222	
1426.885	516.5	194	15.186	
1434.827	5687.12	1914	23.128	$(M+Na)^+$
1450.792	2360.43	791	39.093	$(M+K)^+$
1457.903	8926.47	3028	46.204	
1468.903	30578.6	13088	57.204	
1483.88	503.37	120	72.181	
1490.874	654.53	213	79.175	

1499.859	6532.18	2255	88.16	$(M+ACN+2Na+H)^+$
1508.824	46325.63	22665	97.125	Proline (Pro)
1525.937	9246.7	3311	114.238	TFA
1541.891	2247.39	762	130.192	
1553.903	1031.96	347	142.204	
1555.951	608.07	162	144.252	
1559.905	8114.11	3057	148.206	
1564.9	827.61	260	153.201	
1568.966	2060.58	722	157.267	
1576.883	1982.27	620	165.184	
1581.987	614.85	236	170.288	
1595.87	1026.87	387	184.171	
1621.923	1503.37	458	210.224	
1646.898	771.38	267	235.199	
1655.918	834.12	314	244.219	
1932.128	894.41	385	520.429	
2158.311	643.25	316	746.612	
2287.355	1455.52	757	875.656	
2434.413	4485.97	3179	1022.714	
2530.399	696.22	444	1118.7	
2547.505	68.32	52	1135.806	molecular peak

Table c. Identification of the main picks of CaP(A) of MALDI-TOF

S/N	Intensity	Area	Weight lost (m/z-mass)	Identification
1432.777	77792.81	35243	1.099	$(M+H)^+$
1438.984	988.83	419	7.306	
1440.647	429.02	343	8.969	
1454.764	10251.59	2880	23.086	$(M+Na)^+$
1470.744	1311.71	352	39.066	$(M+K)^+$
1474.793	490.81	123	43.115	$(M+ACN+2H)^+$
1476.752	1564.58	383	45.074	
1488.84	9044.88	2658	57.162	
1503.816	4230.34	1043	72.138	
1510.814	526.11	133	79.136	
1519.811	4483.53	1024	88.133	$(M+ACN+2Na+H)^+$
1538.821	1644.57	359	107.143	
1544.871	529.89	175	113.193	
1548.83	384.54	89	117.152	
1560.845	424.73	118	129.167	DIPEA
1576.839	480.85	127	145.161	
1589.855	484.56	128	158.177	TIS
1610.861	2285.89	556	179.183	
1618.861	4654.88	1294	187.183	
1666.813	1058.79	427	235.135	

1674.901	1391.85	418	243.223	
1684.873	16445.46	5528	253.195	
1706.857	1060.07	320	275.179	
1740.935	1090.58	326	309.257	
1757.934	567.46	172	326.256	
1771.92	404.75	184	340.242	
1786.961	9434.34	3472	355.283	
1834.895	1590.18	518	403.217	
1843.023	1208.75	372	411.345	
1924.024	2961.49	1040	492.346	
2037.109	5059.81	1945	605.431	
2093.175	653.53	234	661.497	
2124.139	521.04	178	692.461	
2502.308	2907.62	1363	1070.63	
2558.37	410.88	192	1126.692	
2856.485	86.55	54	1424.807	molecular peak

Table d. Identification of the main picks of CaP(V) of MALDI-TOF

S/N	Intensity	Area	Weight lost (m/z-mass)	Identification
1417.807	17626.46	4370	1.082	$(M+H)^+$
1439.786	10994.36	2658	23.061	$(M+Na)^+$
1455.759	1200.86	293	39.034	$(M+K)^+$
1461.769	819.95	195	45.044	
1504.835	282.08	52	88.11	$(M+ACN+2Na+H)^+$
1517.866	544.01	114	101.141	Thr o $(DMSO+Na)^+$
1530.895	208.84	40	114.17	TFA
2238.202	766.41	287	821.477	
2352.263	1425.96	585	935.538	
2816.553	170.06	70	1399.828	moleular peak